Sustained Release Behavior of pH-Responsive Poly(vinyl alcohol)/Poly(acrylic acid) Hydrogels Containing Activated Carbon Fibers

Jumi Yun,[1] Ji Sun Im,[1] Young-Seak Lee,[1] Sung Joon Yoo,[2] Hyung-Il Kim[1]

[1]*Department of Fine Chemical Engineering and Applied Chemistry, Chungnam National University, Daejeon 305-764, Korea*
[2]*Bioshield Co. Ltd. 387-33, Gap-Dong, Yusung-Gu, Daejeon 305-323, Korea*

Received 24 February 2010; accepted 20 August 2010
DOI 10.1002/app.33242
Published online 8 November 2010 in Wiley Online Library (wileyonlinelibrary.com).

ABSTRACT: The composites of pH-responsive poly(vinyl alcohol)/poly(acrylic acid) hydrogel and activated carbon fibers (ACFs) were prepared as sustained drug release system with excellent mechanical properties. The mechanical properties of hydrogels were improved greatly by addition of ACFs. The thinner ACFs were more effective in increasing the mechanical properties of composite hydrogels. The cumulative amount of release and the release period were dependent on the surface area and the pore volume of ACFs. The drug release was maximized at basic condition due to the pH-sensitive hydrogel matrices and the initial bust phenomenon was alleviated by incorporating ACFs in the hydrogels. The drug release was sustained about four times longer and the mechanical property was increased about 2.6 times higher because ACFs worked as drug reservoir and reinforcement. Cytotoxicity evaluation confirmed the biocompatible characteristics of the ACFs-containing hydrogels. © 2010 Wiley Periodicals, Inc. J Appl Polym Sci 120: 1050–1056, 2011

Key words: biocompatibility; drug delivery systems; hydrogels; mechanical properties; stimuli-sensitive polymers

INTRODUCTION

Controlled release systems (CRS), which are intended to deliver drugs at predetermined rates for the expected periods, have been used to overcome the drawbacks of conventional drug formulations. In some occasions, it is more beneficial if the drugs are released by the signals from an underlying disease and the necessary amount of drug could be controlled upon the stimulation of such signals. Many researchers have investigated on the stimuli-responsive hydrogels according to the surrounding environment.[1–5]

As a promising candidate material for CRS, hydrogels have been used in the development of the intelligent drug delivery systems.[6,7] Hydrogel has a three dimensional network which is formed by crosslinking polymeric chain of hydrophilic polymers that can swell in water and hold a large amount of water. Hydrogels can not only protect the drug from various hostile environments but also control the release of drug by swelling/deswelling in response to the environmental stimuli. Thus, hydrogels have also been used in various applications such as artificial muscles, drug delivery system, and tissue engineering.[8–12] However, two major drawbacks should be solved for the practical use of hydrogel. First, the poor mechanical properties limit their applications. Even though the mechanical property could be improved by forming the network structure with higher amount of crosslinking agent, the swelling ability would be deteriorated due to the strongly networked polymer structure.[13] As the other drawback, drugs loaded directly into the swollen hydrogels were found to release quickly from the swollen networks.[14–17] Some improvement was also needed in the sustained drug release characteristics for the practical application.

Although the carbon nanotubes (CNTs) were applied for solving above problems, the aggregation of CNTs deteriorated the mechanical properties despite of using surfactant. The high cost of CNTs also limited the extensive application of CNTs.[18–19]

In this study, the activated carbon fibers (ACFs) composite hydrogels were prepared to improve both mechanical properties and sustained release characteristics of hydrogels. ACFs were used as the reinforcing material due to their mechanical and economic advantages.[20,21] ACFs have larger surface area and higher total pore volume for efficient absorption of drugs.[22,23] The effect of ACFs on the controlled release behavior of pH-responsive hydrogel was investigated in terms of sustained release characteristics and mechanical properties.

Correspondence to: H.-I. Kim (hikim@cnu.ac.kr).

EXPERIMENTAL

Materials

ACFs (Adol 10, 15, and 20) were purchased from Osaka Co. (Japan). Poly(vinyl alcohol) (PVA, M_w = 31,000–50,000), acrylic acid (AAc), glutaraldehyde (GA), ethylene glycol dimethacrylate (EGDMA), vitamin B12 (VB12), and potassium persulfate (KPS) were obtained from Sigma Chemical Company.

Drug loading in ACFs

2.0 g of ACFs were immersed in VB12, a model drug, solution (100 ppm, 100 mL) at room temperature for 2 days. VB12-contained ACFs were dried in a vacuum oven for a day at 50°C. 0.5 g of drug-loaded ACFs were put into 100 mL of distilled water to measure the VB12 loading capacity of ACFs.

Preparation of ACFs-contained PVA/PAAc hydrogels

PVA/PAAc hydrogels were synthesized by the free radical polymerization. The polymerization was carried out in de-ionized water using GA and EGDMA as crosslinker of PVA and AAc, respectively. KPS was used as an initiator. The reaction mixture of PVA, AAc, crosslinkers, initiator, and water was stirred for 30 min at room temperature under nitrogen atmosphere. After the reaction mixture was stirred for 2 h at 70°C, various kinds of ACFs (Adol 10, 15, and 20) were added into the reaction mixture. ACFs-contained PVA/PAAc hydrogel (ACH) was prepared after the reaction for additional 2 h. These ACH samples were washed with distilled water at room temperature by replacing with fresh distilled water every few hours. All the ACHs were cut into disc-like pieces having $\sim$ 10 mm in diameter and 10 mm in thickness for the following studies. Swollen hydrogels were completely dried after overnight at 60°C under vacuum. The feed composition of ACHs is summarized in Table I.

TABLE I
Feed Compositions of ACFs-Containing PVA/PAAc Hydrogel (ACH)

	ACH 0	ACH 10	ACH 15	ACH 20
PVA (g)	15	15	15	15
AAc (g)	4	4	4	4
GA (g)	3	3	3	3
EGDMA (g)	1	1	1	1
KPS (g)	0.2	0.2	0.2	0.2
Adol 10 (g)	–	2.0	–	–
Adol 15 (g)	–	–	2.0	–
Adol 20 (g)	–	–	–	2.0

Characterization

Swelling behavior

Three different kinds of pH buffers (2, 7, and 10) were used as swelling media and the swelling behaviors were determined by gravimetric method. The dried samples were immersed into the various pH buffer solutions for a certain period until the swelling equilibrium was reached and then these hydrogels were taken out for wiping with tissue paper to remove excess buffer solution on the surface. They were weighed immediately. The equilibrium swelling ratio (%) of the hydrogels was calculated as follows:

$$\text{Swelling } (\%) = (W_s - W_d)/W_d \times 100$$

where W_d and W_s are the weights of dry and swollen samples, respectively.

Morphology

The morphologies of samples were investigated using field emission scanning electron microscopy (FE-SEM) apparatus (JEOL, JSM-7000F). As a pretreatment, the samples were vacuumed up to 10^{-3} Pa and sputtered with Pt.

Pore structure of ACFs

To investigate the pore structures such as specific surface area, pore volume, and micropore fraction, BET apparatus (ASAP 2020) was used. ACFs were degassed up to 10^{-3} Pa and then, nitrogen gas (99.9999%) adsorption was carried out at 77 K. Specific surface area was calculated by using BET equation and micropore volume was measured by HK (Horvath-Kawazoe) method.

Mechanical properties

The mechanical properties of ACHs were measured by an Instron tester model 5583 at 25°C and 50% relative humidity with a compression load cell, having a full-scale range of 1.0 KN. All the samples were immersed in water at room temperature for 3 days to reach the equilibrium state of swelling. Swollen samples were then placed on the top plate of a compression load cell and compressed by a cylindrical metal rod probe (diameter 10 mm) at a constant crosshead speed of 2 mm/min until the fragmentation of the sample occurred. Initial compression modulus was calculated from the initial slope of the stress–strain curve.

Release behavior

VB12 release from ACHs was carried out in pH 2, 7, and 10 buffer solutions. The amount of VB12 was

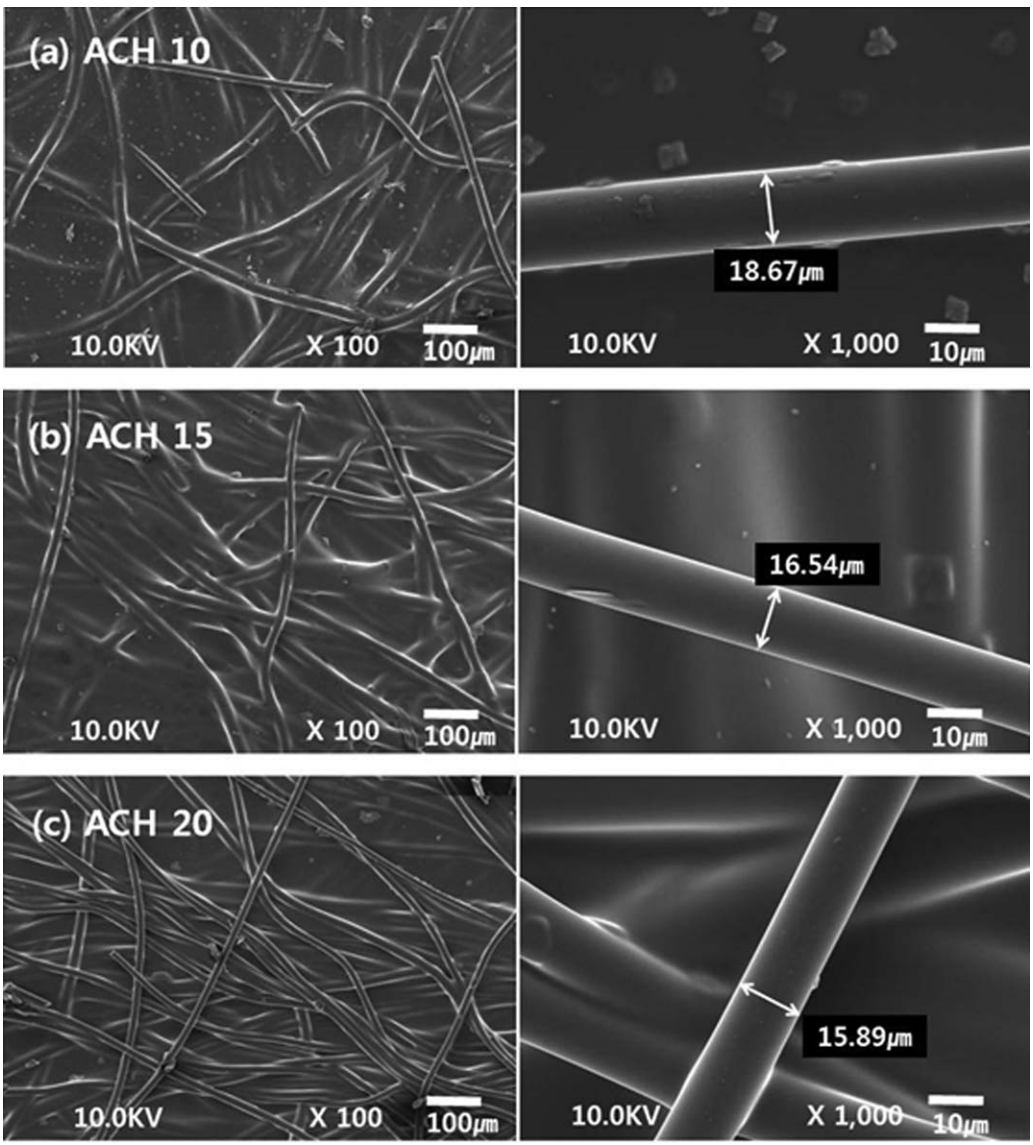

Figure 1 SEM images of various ACHs. (a) ACH 10, (b) ACH 15, and (c) ACH 20.

measured at various time periods using a UV spectrometer (Optizen 2120 UV, Mecasys, Korea). The buffer solution was refreshed after sampling. All the experiments were carried out in triplicate.

The cumulative release of VB12 was calculated as follows:

$$\text{Cumulative release } (\%) = (M_t/M) \times 100,$$

where *Mt* is the cumulative amount of VB12 released from the ACH at time *t* and *M* is the total amount of VB12 preloaded in ACFs.

Indirect cytotoxicity evaluation

The indirect cytotoxicity evaluation of samples was carried out by using Cell Counting Kit-8 (CCK-8), which was purchased from Dojindo Laboratory, Japan. Experimental design was conducted according to the ISO10993-1, 5, and 12 standard test methods.[24] The samples were taken to 0.1 g. The extraction media were prepared by immersing the samples in a 96-well microtiter plate at 5×10^3 cells/well and incubated for 24 h. Mouse fibroblasts (L 929, KCLB No 10001) were seeded in a 96-well plate at a density of 5×10^3 cells/well and incubated at 37°C under a 5% CO_2 humidified atmosphere in DMEM (Dulbecco's Modified Eagle's Medium) containing 10% FBS (Fetal Bovine Serum) and penicillin (5000 U/mL)/streptomycin (50 μg/mL). The culture medium was removed after 24 h and then the prepared extraction media was added to the 96-well. The cells were incubated for 24 h and the number of viable cells was quantified with the CCK-8 (Cell Counting Kit-8). The absorbance of CCK-8 was measured at 450 nm using an automated ELISA (enzyme linked

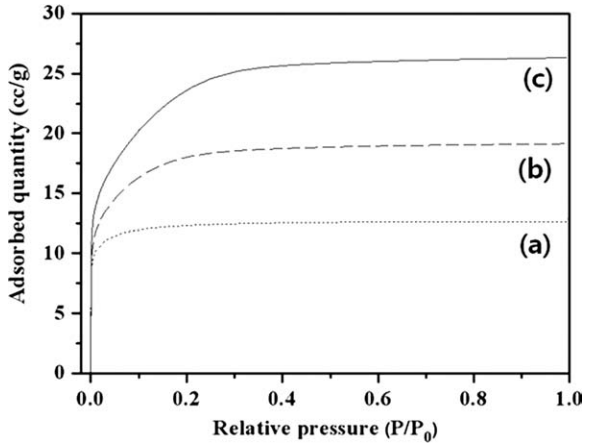

Figure 2 Nitrogen isotherms of various ACFs. (a) Adol 10, (b) Adol 15, and (c) Adol 20.

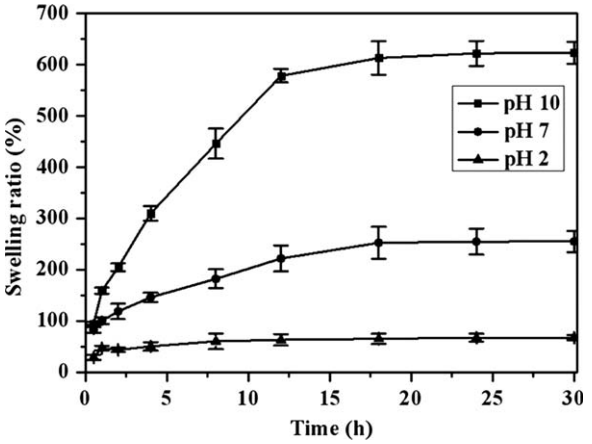

Figure 3 Swelling behavior of ACH 20 in various pH buffers.

immunosorbent assay) microplate reader (Bio-Tek Instruments, Winooski). The analysis was carried out in triplicate.

RESULTS AND DISCUSSION

Morphology investigation

The SEM images of ACHs are presented in Figure 1. ACFs were found in the PVA/PAAc hydrogel matrix to form a new system: fibers in hydrogel, although some ACFs were aggregated. The measured diameters of Adol 10, 15, and 20 were 18.67, 16.54, and 15.89 μm, respectively. Some of carbons on the surface of fiber were removed as CO or CO_2 during activation process resulting in decreased diameter of fiber.[25] Thus, the fiber having the higher pore structure usually showed the smaller diameter of fiber. ACFs were uniformly distributed without noticeable variation in surface morphology. ACFs were incorporated physically into PVA/PAAc hydrogel matrix without strong interactions between ACFs and PVA/PAAc matrix.

Pore structure

Nitrogen isotherms of ACFs were obtained to investigate the pore structure as shown in Figure 2. Generally, the isotherm curves in the relative pressure of less than 0.1 indicates the adsorption in the micro pore and the isotherm curve in the relative pressure over 0.1 is related to the adsorption in the meso and macro pores.[26] All the ACFs had mainly the micro pore structures based on the significant changes in the relative pressure range of less than 0.1 as shown in Figure 2. The amount of adsorbed nitrogen increased in the order of Adol 10, 15, and 20 reaching 12.5, 17.5, and 25.0 cc/g, respectively. Less significant changes in the relative pressure over 0.1 indicated that ACFs had negligible contents of meso and macro pores.

The structural characteristics of Adol 10, 15, and 20 were summarized in Table II. The specific surface areas and total pore volumes varied depending on the kinds of ACFs. All the ACFs had micro pore volume fraction of over 90%. These micro pores seemed to play important role in the sustained release of VB12 which was loaded in ACFs.

TABLE II
Structural Characteristics of ACFs (Adol 10, 15, and 20)

	Adol 10	Adol 15	Adol 20
S.S.A. (m^2/g)	9.26×10^2	1.63×10^3	1.92×10^3
T.P. (cm^3/g)	4.37×10^{-1}	8.23×10^{-1}	8.74×10^{-1}
M.P. (cm^3/g)	4.26×10^{-1}	7.46×10^{-1}	8.48×10^{-1}

S.S.A., specific surface area; T.P., total pore volume; M.P., micro pore volume.

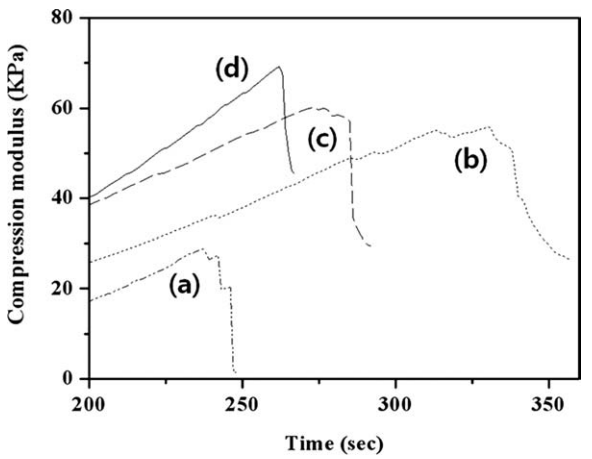

Figure 4 Compression moduli of various ACHs depending on time. (a) ACH 0, (b) ACH 10, (c) ACH 15, and (d) ACH 20.

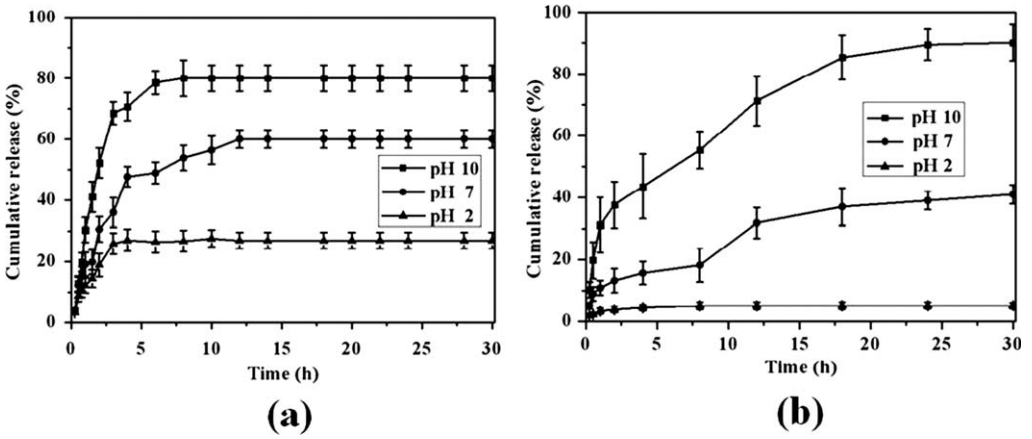

Figure 5 Drug release behavior of ACHs in various pH buffers. (a) ACH 0 and (b) ACH 20.

Swelling behavior

The pH-sensitive swelling behavior of ACHs is presented in Figure 3. The swelling of ACHs increased greatly as the pH of buffer solution increased. PVA/PAAc hydrogels have pendant carboxylic acid groups which can be ionized into carboxylate anion above its pKa of 4.7. The amount of carboxylate anion increased as the pH increased. The carboxylate anions cause more electrostatic repulsion and hydrophilicity to the polymer chains. Therefore, PVA/PAAc hydrogels show the pH-sensitive swelling behavior. The drug release can be accelerated by the swelling characteristics of PVA/PAAc hydrogel especially at higher pH.

Mechanical properties

The mechanical properties of ACHs were evaluated by the compression modulus as shown in Figure 4. The mechanical strength of ACHs increased greatly by incorporation of ACFs into the hydrogel matrix. The mechanical strength of ACHs increased noticeably as the ACFs had the lower diameter due to the increased ACFs concentration effect. This is well matched with the previous result that fibers with smaller diameter and higher concentration can increase the mechanical property of matrix more effectively than using thicker fiber with lower concentration.[27]

Sustained release behavior

The sustained release behavior was studied for both PVA/PAAc hydrogel matrix (ACH 0) containing VB12 inside and ACH 20 containing VB12 in the ACFs. The pH-sensitive release behavior of both samples is well presented in Figure 5. The cumulative amount of released VB12 increased in a basic buffer solution due to the higher swelling of PVA/PAAc hydrogel matrix. The surface morphology of the freeze-dried PVA/PAAc hydrogel matrix was observed by SEM as shown in Figure 6. The expanded surface texture was detected for the hydrogel swollen in the buffer solution of pH 10 due to the extensive swelling of hydrogel matrix. These morphological changes are believed to result in the variation of both release rate and cumulative amount of release from the hydrogel. The significant difference between ACH 0 and ACH 20 in VB12release behavior is found in Figure 5. The release of VB12 was completed only in 5 h for ACH 0.

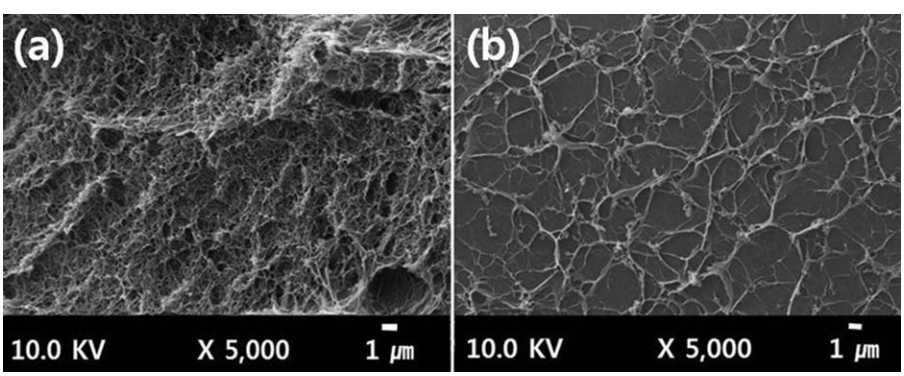

Figure 6 SEM images of freeze-dried ACH 20 swollen in different buffers. (a) pH 2 and (b) pH 10.

However, VB12 was released in a sustained manner to 30 h for ACH 20 because ACFs controlled the release of VB12 which was loaded in the micro pores.

The cumulative amounts of released VB12 are shown in Figure 7. The total amount of VB12 loading was less in PVA/PAAc hydrogels containing ACFs because VB12 was loaded not in the hydrogel matrix but in the micro pores of ACFs, whereas VB12 was loaded only in the hydrogel matrix for ACH 0. The improvement in sustained release behavior is clearly noticed in the ACFs-contained PVA/PAAc hydrogels regardless of the kind of ACFs. The release of VB12 depended on not only the swelling of PVA/PAAc hydrogel matrix but also the type of ACF reservoir. The incorporation of ACFs, which was used as a reservoir for the drug loading, worked successfully for the sustained release behavior in addition to the pH-responsive properties of hydrogel matrix. Although the sustained drug release was reported by using special treatments such as graft-polymerization and ionic or hydrophobic interaction between drug and polymers,[28–31] the excessive reaction time and cost were needed. On the other hand, the incorporation of ACFs in the drug release matrices provides easy way to control the release of drug. The improvement in the sustained release of drug could be achieved by releasing the drug through two kinds of interfaces, ACF/drug and hydrogel/drug, having different drug release thresholds.

Cytotoxicity test

The cytotoxicity test was carried out to investigate the biocompatibility of ACHs as shown in Figure 8.

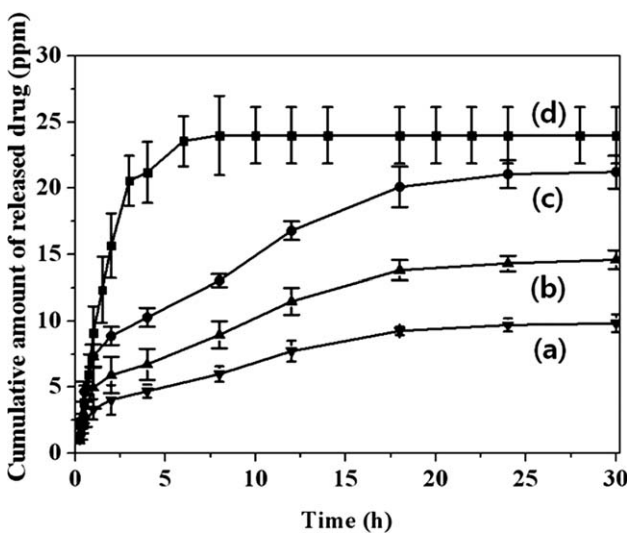

Figure 7 Cumulative amount of released VB12 from various ACHs at pH 10. (a) ACH 10, (b) ACH 15, (c) ACH 20, and (d) ACH 0.

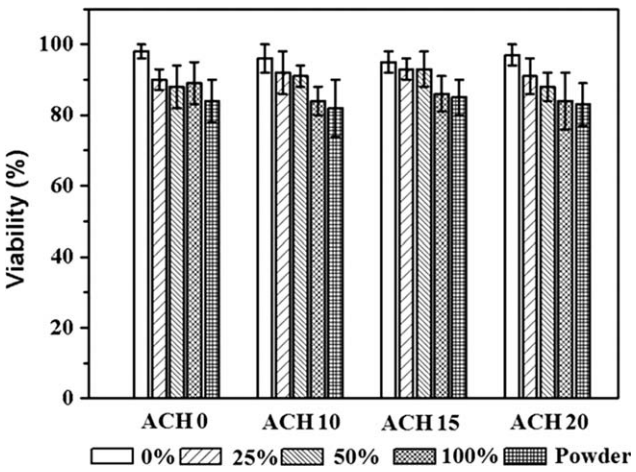

Figure 8 Variation of viability of mouse fibroblast L929 cells in various ACHs depending on the content of extract from ACHs in saline solution. Powder stands for ACHs before extraction in saline solution.

All the ACHs showed the high viability over 80%. Therefore, all ACHs samples are nontoxic with high cell viability and ACHs could be applied to the sustained drug delivery system without causing any cytotoxic problem.

CONCLUSIONS

The hydrogels, having interpenetrating network of PVA, pH-responsive PAAc, and ACFs, were prepared by a radical polymerization. The mechanical properties of PVA/PAAc hydrogel increased significantly by incorporation of ACFs. The VB12-loading capacity and releasing characteristics of ACFs varied depending on the surface area and micro pore volume of ACFs. PVA/PAAc hydrogels showed the reversible swelling behavior depending on the pH variations. PVA/PAAc hydrogels swelled rapidly in the basic buffer solution. The extensively swollen hydrogel was responsible for the faster release rate and the larger release amount of VB12 in the basic condition. Controlled release of VB12 from ACFs, which were distributed in the PVA/PAAc hydrogel matrix, resulted in the sustained release system. ACFs played important role in maintaining the constant release rate for 30 h. The release of VB12 could be controlled easily both by the pH-responsive hydrogel matrix and the ACF reservoir.

References

1. Ko, J. A.; Park, H. J.; Hwang, S. J.; Park, J. B.; Lee, J. S. Int J Pharm 2002, 249, 165.
2. Kortesuo, P.; Ahola, M.; Kangas, M.; Jokinen, M.; Leino, T.; Vuorilehto, L.; Laakso, S.; Kiesvaara, J.; Yli-Urpo, A.; Marvola, M. Biomaterials 2002, 23, 2795.
3. Palmieri, G. F.; Bonacucina, G.; Martino, P. D.; Martelli, S. Int J Pharm 2002, 242, 175.

4. Yun, J.; Im, J. S.; Oh, A.; Lee, Y. S.; Kim, H. I. Carbon Lett 2009, 10, 33.
5. Yun, J.; Im, J. S.; Jin, D.; Lee, Y. S.; Kim, H. I. Carbon Lett 2008, 9, 283.
6. Martin, G. R.; Jain, R. K. Cancer Res 1994, 54, 5670.
7. Qiu, Y.; Park, K. Adv Drug Deliv Rev 2001, 53, 32.
8. Osada, Y.; Okuzaki, H.; Hori, H. Nature 1992, 355, 242.
9. Hoffmann, J.; Plotner, M.; Kuckling, D.; Fischer, W. J Sens Actuators A Phys 1999, 77, 139.
10. Bassil, M.; Davenas, J.; Tahchi, M. E. L. Sensors Actuators B 2008, 134, 496.
11. Shinji, S.; Hirose, K.; Taguchi, K.; Ogushi, Y.; Kawakami, K. Biomaterials 2009, 30, 3371.
12. Liu, Y.; Bharadwaj, S.; Lee, S. J.; Atala, A.; Zhang, Y. Biomaterials 2009, 30, 3865.
13. Peppas, N. A. Biomaterials Science: An Introduction to Materials in Medicine; Elsevier: Toronto, 1996.
14. Hoffman, A.; Afrassiabi, A.; Dong, L. J Controlled Release 1986, 4, 213.
15. Bae, Y.; Okano, T.; Hsu, R.; Kim, S. Macromol Chem Rapid Commun 1987, 8, 481.
16. Zhang, X.; Zhuo, R.; Cui, J.; Zhang, J. Int J Pharm 2002, 235, 43.
17. Zhang, X.; Wu, D.; Chu, C. Biomaterials 2004, 25, 3793.
18. Spitalsky, Z.; Tasis, D.; Papagelis, K.; Galiotis, C. Prog Polym Sci 2010, 35, 357.
19. Im, J. S.; Kim, S. J.; Kang, P. H.; Lee, Y. S. J Ind Eng Chem 2009, 15, 699.
20. Kanawade, D.; Jandali, G.; Mallick, P. K.; Development of Thermoplastic Matrix Composite Tubes for Automotive Applications; Presented at the Proceedings of the 17th Technical Conference of the American Society for Composites, West Lafayette, 2002.
21. Morgan, P. Polymer Matrices for Carbon Fiber Composites: Carbon Fiber and Their Composites; Taylor & Francis: New York, 2005.
22. Im, J. S.; Jang, J. S.; Lee, Y. S. J Ind Eng Chem 2009, 15, 914.
23. Jung, M. J.; Kim, J. W.; Im, J. S.; Park, S. J.; Lee, Y. S. J Ind Eng Chem 2009, 15, 410.
24. Sangsanoh, P.; Waleetorncheepsawat, S.; Suwantong, O.; Wutticharoenmongkol, P.; Weeranantanapan, O.; Chuenjitbuntaworn, B.; Cheepsunthorn, P.; Pavasant, P.; Supaphol, P. Biomacromolecules 2007, 8, 1587.
25. Im, J.; Park, S.; Kim, T.; Kim, Y.; Lee, Y. J Colloid Interface Sci 2008, 318, 42.
26. Im, J. S.; Park, S. J.; Lee, Y. S. J Colloid Interf Sci 2007, 314, 32.
27. Thomason, J. L. Compos A 2008, 39, 1732.
28. Siemoneit, U.; Schmitt, C.; Alvarez-Lorenzo, C.; Luzardo, A.; Otero-Espinar, F.; Concheiro, A.; Blanco-Méndez, J. Int J Pharm 2006, 312, 66.
29. Alvarez-Lorenzo, C.; Concheiro, A. J Controlled Release 2002, 80, 247.
30. Alvarez-Lorenzo, C.; Concheiro, A. J Chromatogr B 2004, 804, 231.
31. Jimenez-Kairuz, A.; Allemandi, D.; Manzo, R. Int J Pharm 2003, 250, 129.